Decentralized Fuzzy Logic Control of Microgrid for Electric Vehicle Charging Station

Pablo García-Triviño, Juan P. Torreglosa, Luis M. Fernández-Ramírez, *Senior Member, IEEE*, and Francisco Jurado, *Senior Member, IEEE*

***Abstract*— As already happens with the electric vehicles (EVs) expansion, technology associated with their charge also must be improved. This paper presents a novel decentralized control method for charging stations based on a medium-voltage direct-current (MVDC) bus. This kind of charging stations is integrated in a microgrid with a PV system, a battery energy storage system, a local grid connection and two units of fast charge. The main contribution of this work resides in the cited decentralized control method based on fuzzy logic that includes the state of charge of the battery energy storage system as a control variable. This control contains two independent fuzzy logic systems (one for the battery energy storage system and other for the grid), whose function is to maintain the MVDC voltage and the battery energy storage system state-of-charge within proper thresholds and to keep the power balance stable among the units of fast charge and the rest of the charging station components. The new control method was tested in a considerable number of operating situations (two hundred cases studied) under different conditions of sun irradiance, initial state-of-charge of battery energy storage system and number of EVs connected to the charging station with the objective of showing its correct performance in all the considered scenarios.**

***Index Terms*— Electric vehicle; energy storage; fuzzy logic; photovoltaic systems.**

I. Introduction

Currently, due to climate change and high dependence on fossil fuels in the transport sector [1] most of the countries have created new and more demanding laws to regulate and control issues related with CO_2 and NOx emission [2]. The promotion of plug-in hybrid electric vehicles (PHEVs) and electric vehicles (EVs) is a clearly feasible solution to cope with this problem [3]. Nowadays, some manufactures guarantee an autonomy of their EVs around 500 kms or even more. Besides, if a thermal power plant is assumed as the origin of the power, the overall EV efficiently is at least twice respect to internal combustion engine (ICE) vehicles [4]. Nevertheless, the technology associated to them, specially related to the EV charging stations (CSs), needs to be developed deeply. CSs have to be distributed in the cities and supply fast charging to the EVs, which involves a high electricity demand. The local electrical grid has to be able to withstand this high power demand and the problems related with the connection of DC systems (harmonics, voltage outages, and fluctuations) [4-6].

On the other hand, as stated in [7], other challenges still exist to their large scale implementation: EVs acquisition costs are higher than the ICE ones; limited public charging infrastructure; an increase of the power demand to the grid (worsened in case of short charging). Therefore, rising up the power generation with renewable energy sources and scheduling the charging profiles of different EVs are proposed as solutions. Both are strictly related to a deployment of smart-grid technologies, such as smart meters, information and communication technology and energy storage systems (ESSs). Since 2012, the installation of fast CSs has increased eight times while the number of normal chargers only has doubled [8]. For this kind of CSs, ESSs become fundamental, since they can provide peak shaving and power quality functions and also make the charge time shorter.

According to the IEC 61851-1 Committee on "Electric vehicle conductive charging system" [9], there are four modes of charging depending on the quantity of power received by the EV, the type and level of voltage, the communication mode between the CS and the EV, and the location of the protections. This paper is focused on the Mode 4 (DC level 2): fast charging using an external DC charger with a rated power of 100kW.

There is a growing number of works related to CSs from a wide range of research approaches. They can be classified in three groups: EV charging scheduling, control of the CS power converters and power flow in CSs.

Charging scheduling studies consider a framework of long-term/electricity market. The focus of this kind of papers is the effect of CSs in the power grid and they deal with the scheduling problem as an optimal power flow problem. The

Manuscript received February 01, 2017; revised July 30, 2017; revised July 30, 2017; revised November 18, 2017; accepted January 02, 2018. This work was partially funded by the Spanish Ministry of Economy and Competitiveness under Grand ENE2013-46205-C5-1-R.

P. García-Triviño and L. M. Fernández-Ramírez are with the Research Group in Electrical Technologies for Sustainable and Renewable Energy (PAIDI-TEP-023), Department of Electrical Engineering, Higher Polytechnic School of Algeciras, University of Cadiz, 11202 Algeciras, Spain (e-mail: pablo.garcia@uca.es; luis.fernandez@uca.es).

J. P. Torreglosa is with the Department of Electrical Engineering, University of Huelva, Carretera Palos-Huelva, s/n. 21071 Palos de la Frontera, Huelva, Spain (email: juan.perez@die.uhu.es).

F. Jurado is with the Research Group in Research and Electrical Technology (PAIDI-TEP-152), Department of Electrical Engineering, Higher Polytechnic School of Linares, University of Jaén, 23700 Linares, Spain (e-mail: fjurado@ujaen.es).

capability of EVs of storing energy can provide great flexibility and benefit both EVs and grid. With this premise, some works have studied EV charge scheduling by means of simulations [10-14]. In [10], the scheduling problem was studied considering the vehicle-to-vehicle (V2V) mechanism. The integration of renewable energy sources as additional power supply for CSs was studied in [11]. Other examples of this kind of works are [12, 13] that studied vehicle-to-grid (V2G) mechanism that enabled EVs to transfer energy back to the power grid. Both V2G and V2V functionalities were considered in [14], in a grid-connected and PV supplied charging park. The models and simulations presented in them used sampling time periods whose duration lasted from minutes to hours. Thus, the dynamics of fast charging were neglected.

On the opposite side, the approaches focused on CS power converters control require small sampling time periods and detailed models to study the interaction among the CS and the utility grid. Some works that can be classified in this group are [15-17]. In them, the simulations and experimental test consisted on study the performance of the converter under steady state conditions and under transitions between different operation modes. These transitions were governed by energy management systems (EMSs) in charge of controlling the power flow among the components of the CS. However, since the simulation and experiment intervals were short, the EMS was not considered in this kind of works and its commands were replaced by standardized control inputs such as step signals.

The third group corresponds to the works focused on controlling the power flow among the components of the system. In them, there must be a compromise between the model accuracy and the experiments length. Thus, it is common to model the converters as average models that can provide a reasonably accurate representation of low order harmonics preserving the dynamics resulting from the control system and allowing longer simulations. The number of this kind of publications found after a review is less than in the previous groups [3, 18-22]. All of them have in common a topology based on a DC bus that all the power converters are connected to. In [3], it was validated, by means of laboratory experimental tests, the practical feasibility of a centralized control strategy previously tested by simulations in [18]. The switching between the modes of operation occurred due to the changes in the voltage level at the DC link as a result of changes in the irradiation on the PV panel. Another PV based battery switch CS was simulated in MATLAB in [19]. Its main objective was to ensure the service availability improving the PV energy self-consumption. Again, since the sampling period taken was 1 minute, dynamics of the power converters were neglected. In [20], it was proposed a distributed control whose decision parameter was the DC bus voltage. The modelling technique followed by this study was based on reduced order small-signal stability models from which real-time simulation results were collected to verify the control method proposed. In [21], the CS, as novelty, contains a Superconducting Magnetic Energy Storage (SMES). The centralized controller consisted in a simple power balance: under steady state conditions, the EVs were charged by the power generated by the PV panels and the difference was supplied by the grid. SMES only worked during transitory conditions to mitigate the effect of rapid charging as power peaks across the network. However, the State-Of-Charge (SOC) of the SMES was not taken into account in the EMS. The research presented in [22] developed a centralized controller for a CS, whose objective was to minimize the operating cost of the system. It was composed by 3 layers: a weather and EV charging forecasting stage; a Particle Swarm Optimization (PSO) algorithm to minimize the daily running cost of the CS; and a dynamic programming for keeping the battery SOC within the specified limits. The interval periods used for the simulations varied from 10 minutes to one hour and were used to verify the effectiveness of the proposed EMS. However, the long interval periods of the simulations were not suitable to study the dynamics of DC bus voltage that, instead, were studied by experimental tests.

The work presented here belongs to the last group and shares with the commented works the topology based on DC bus. With regard to the EMS, the majority of works [21, 22] proposed centralized controllers that are suitable for small CSs, whose components are placed in a close location. A decentralized control was developed in [20], which allows to easily expand the system adding more power sources, ESS and EV chargers forming a Medium Voltage (MV) microgrid. The novelty of this work with regard to previous decentralized EMS was to include the SOC of the ESS as a control variable in the control strategy that must be kept within proper limits. This is a common approach in centralized strategies [21, 22], whose components are connected by a communication network but it is difficult to deploy for decentralized systems. Regarding to the detail of the models employed previously, for both centralized and decentralized commented strategies, they were simplified since the objective of the studies was to check that the strategies resulted in a proper power flow among the CS components. The effects of the strategies in parameters such as DC bus voltage or current sharing were studied from data collected from experimental test, since the complexity of the models was not enough to represent power converters dynamic. Besides, another novelty is that the different power converters have been modelled as average models that result in simulations that represent more reliably the CS dynamics improving the approaches followed before in this area. In this work, the Decentralized Control Method (DCM) proposed is based on fuzzy logic systems, which is in charge of the power flow management of a CS.

Fuzzy systems have been applied to a large variety of fields of knowledge because of its easy adaptability to complex systems and the lack of need for historical data as required by other intelligent controllers. For these reasons, fuzzy logic control has been used in this work. Other examples of its usage for EMS in EV CSs were presented in [23-25]. ¿Other examples not related with the energy management appeared in [26, 27] for determining the charging or discharging priority of each EV and fault diagnosis in plug-in hybrid EVs,

This article has been accepted for publication in a future issue of this journal, but has not been fully edited. Content may change prior to final publication. Citation information: DOI 10.1109/JESTPE.2018.2796029, IEEE Journal of Emerging and Selected Topics in Power Electronics

respectively. Apart from that, fuzzy logic is also a good tool as a controller for power converters of CSs [28-30]. The main novelty of the present work against the commented is the use of fuzzy controllers as a decentralized EMS to control the converters of two elements of the system separately and achieve a coordinated operation of the following parameters: power flow, MVDC voltage and BESS SOC. Thus, it can be said that this control method combines two of the application areas of the fuzzy logic in this field. Finally, this novel decentralized control has been evaluated and analysed in a considerable number of operating situations, in contrast to the previous works published on this topic, in order to perform a sensitivity and stability analysis of the proposed control technique and show how the components of the system interact. Monte-Carlo simulations (two hundred simulations of ten second each) have been carried out and analysed, in which the PV power, the number EV connected and the initial BESS SOC have been modified randomly in order to know the control results and the response of the whole system under study.

The structure of this paper is as follows. After the introduction, the configuration of the microgrid for EVCS is described in Section II. Section III is dedicated to the description and modelling of the microgrid components. Section IV develops the DCM based on fuzzy logic systems for the BESS and grid power converters. Section V, Simulation Results, presents the scenario considered for this study, the performance of the proposed fuzzy logic based DCM compared with a simpler DCM based on PI controllers, and a sensitive and stability analysis of the results obtained by the fuzzy logic based DCM. Finally, the conclusions are drawn in Section VI.

II. Microgrid for Electric Vehicle Charging Station

The microgrid for electric vehicle changing station (EVCS) under consideration in this paper (Fig. 1) consists of a PV system with a peak power of 120 kWp [31] as renewable energy source, a battery AES from Discover Energy [32] with a rated capacity of 23.9 kWh as BESS, two units of fast charge (48kW each one) based on Li-ion batteries from Xalt Energy [33], and a connection system with the grid. The units of fast charge are defined as Mode 4, DC level 2 according to the IEC 61851-1 (fast charging with external charger in DC, voltage inferior to 500V and current inferior to 200A) so, accordingly, each unit of fast charge has a DC/DC converter for controlling the charging of the EV. Besides, to assure high power supply to the EVCS and the simultaneously charging of the units of fast charge, all these components are connected to a 1500V DC bus (MVDC bus). DC/DC converters are used for the BESS and PV system in order to adapt the DC bus voltage to the output voltage of these components and controlling their power flow. The connection with the grid is composed of a transformer and a bidirectional DC/AC converter.

The control presented in section III must keep the MVDC bus voltage, manage the power balance among the components and control the BESS SOC. All these actions must be carried out without a centralized system that collects

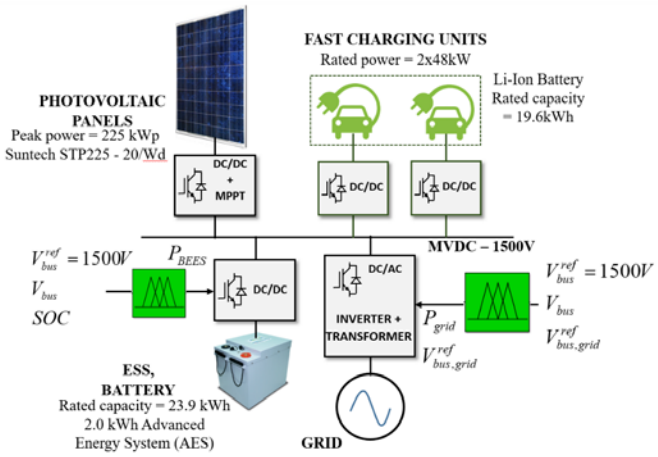

Fig. 1. Microgrid for the EVCS under study.

the most important parameters of each element, and according to these data, generates the reference power of each component. Instead of this kind of control, a DCM based on independent fuzzy logic controllers is designed. Thanks to this configuration, each component can operate independently without knowing the status of the rest of the system, alleviated the theoretical and practical limitation of power supply reliability, which can help to facilitate large distribute generator access [34].

III. Description and Modelling of the Components

This section describes the components used in the microgrid and their modelling by models widely used in scientific literature. In fact, the PV system, the batteries of ESS and EVs, the power converters and the EVs charging method are described below. Fig. 2 depicts the models used for the components of the microgrid and Table I shows the main parameters of these components. Fig. 3 shows the comparison between the curves obtained from the models and real components (real curves provided by commercial datasheets) for the PV system and batteries of ESS and EVs under study. The results reflect an accurate approximation of the real results achieved by the models.

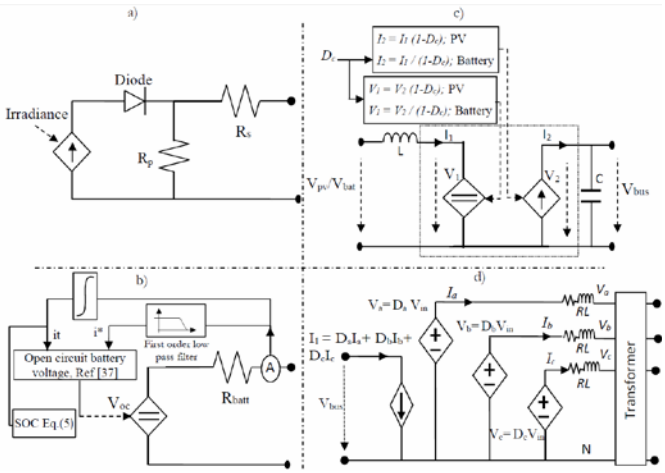

Fig. 2. Models for: a) PV system. b) ESS and EV batteries. c) DC/DC converter. d) Grid connection.

This article has been accepted for publication in a future issue of this journal, but has not been fully edited. Content may change prior to final publication. Citation information: DOI 10.1109/JESTPE.2018.2796029, IEEE Journal of Emerging and Selected Topics in Power Electronics

TABLE I.
MAIN PARAMETERS OF THE MICROGRID MODEL

Paramenter	*Value*
PV system converter, L	$0.45\text{x}10^{-3}$ H
PV system converter, C	$215\text{x}10^{-6}$ F
PV model, Ns	0.9 Ω
PV model, Np	235 Ω
Filter, R	1850 Ω
Filter, L	$250\text{x}10^{-6}$ H
ESS battery model, R_{batt}	0.15 Ω
ESS battery converter, L	$0.4\text{x}10^{-3}$ H
ESS battery converter, C	$22\text{x}10^{-6}$ F
EV battery model, R_{batt}	0.07 Ω
Fast charging unit converter, L	$1.1\text{x}10^{-3}$ H
Fast charging unit converter, F	$40\text{x}10^{-6}$ F

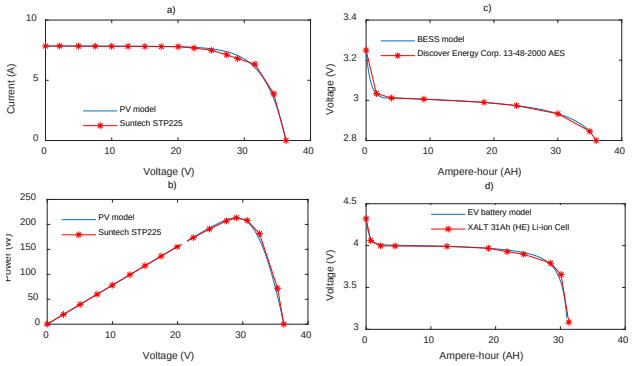

Fig. 3. Validation of the models by comparing the characteristic curves obtained from the model and real component for the PV system and batteries of ESS and EVs.

A. PV System

The PV system model used for the case study is based on a controllable current source, a diode, a series resistance R_s and a parallel resistance R_p (Fig. 2a). This model, already tested in several papers [35, 36], is known as the single-diode model of a PV array. The output current of this model (I_{pv}) is calculated through the next expression.

$$I_{pv} = I_{ph} - I_{sat}\left(e^{q\left(V_{pv}+I_{pv}R_s\right)/\left(NkT_{pv}\right)}\right) - \left(V_{pv}+I_{pv}R_s\right)/R_p \quad (1)$$

where I_{ph} is the solar-induced current and I_{sat} is the saturation current of the diode. The next expressions show the calculation of these currents.

$$I_{ph} = I_{ph0}\left(1+K_0\left(T_{pv}-300\right)\right) \quad (2)$$

$$I_{sat} = K_1 T^3 e^{\left(-\frac{qV_g}{kT_{pv}}\right)} \quad (3)$$

Other parameters of the above expressions are the following ones: V_{pv} is the PV output voltage, I_{pho} is the solar-induced current at 300 ºK; K is the Boltzmann constant; K_o and K_1 are constants depending on the PV characteristics [36]; N is the quality factor of the diode of the PV model; q is the elementary charge of an electron; V_g is the voltage applied to the terminals of the diode; and T_{pv} is the PV operating temperature.

Apart from that, a DC/DC converter, modelled as commented in section III.D adapts and controls the output voltage of the PV system to work at the MPPT mode.

B. EV and ESS Batteries

The battery technology used for this study is Li-ion for both the EV and the ESS. Currently, the most used battery type for EVs is Li-ion. In the case of the ESS for CS there is a lack of information, so the choice has been made based on two points supported by [7]: Li-ion batteries have a very high efficiency (85–95%), high energy density, and high number of life cycles (3.000–5.000); and Li-ion batteries as ESS have been already used in a real implementation of an EV fast CS [7], whose experimental test results showed that the system has a good performance.

The battery model from SimPowerSystems toolbox of Simulink [37] has been selected to model the batteries of the EVs and ESS (see Fig. 2b), adapting their parameters to the available data provided by their commercial datasheets [32],[33]. A variable voltage source and a series resistance compose this model. Hence, the output battery voltage, V_{bat}, is the difference between the open circuit battery voltage, E_{bat}, and the drop voltage in the internal battery resistance, R_{int} (see Eq. (4)). The method of calculating E_{bat} and the value of R_{int} depend on the type of the selected battery [37].

$$V_{bat} = E_{bat} - I_{bat}R_{\text{int}} \quad (4)$$

The battery SOC is obtained using the simple Coulomb-counting approach (Eq. (5)), where the maximum battery capacity is denoted as Q.

$$SOC(\%) = SOC_o(\%) - 100\left(\frac{\int I_{bat}\cdot dt}{Q}\right) \quad (5)$$

It was demonstrated in [38] that the dynamic behavior of this battery model obtained in simulation is close to the experimental behavior, with low errors for SOC between 100% and 20% during the charging and discharging mode. In fact, the control implemented in this work allows the battery to work with a SOC between 20% (to avoid deep discharging) and 100%. Coulomb-counting approach for calculating the SOC is widely used because the required computational power is low [39]. Furthermore, its performance with Li-ion battery (the kind of battery used in this work) is better than with other types of batteries due to the lower magnitude of side reactions. The main disadvantage of this method is the cumulative error in the current integration. The accuracy of this method is determined by the current sensor accuracy (and also by the test duration and capacity knowledge). When this method is run over a long period of time, significant inaccuracy arises from accumulated current measurement errors. However, since only simulations are presented in this work, the inaccuracy of the current measurement is neglected and thus, the inaccuracy of SOC.

C. EV Charging

The EV charging can be performed by means of several methods: pulse charge, constant voltage (CVM), constant current mode (CCM), constant power mode (CPM), among others. In the case of charging Li-ion batteries for EVs, a combination between two of them (CCM and CVM) is becoming the most suitable alternative [40]. Reduction of the

This article has been accepted for publication in a future issue of this journal, but has not been fully edited. Content may change prior to final publication. Citation information: DOI 10.1109/JESTPE.2018.2796029, IEEE Journal of Emerging and Selected Topics in Power Electronics

charging time and better control of the maximum battery voltage are its main advantages. Thus, this method is used to perform the charging of EVs [41].

In the CCM, the EV is charged with a constant current value (I_{char}) while, in the CVM, a constant voltage value (V_{char}) is applied to the EV. Thus, if an EV is connected to a charging unit with a battery voltage lower than V_{char}, the EV will be charged in the CCM, and therefore, its voltage level will increase. Once the EV battery voltage reaches V_{char}, the EV will skip to the CVM and the battery input current will

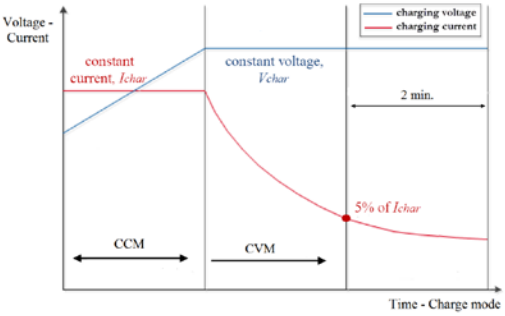

Fig. 4. Charging modes for the EV.

progressively decrease. The charging of the EV will end when the charging current is lower than 5% of I_{char} during 2 min. Fig. 4 shows a scheme of this charging method.

D. Power Converters

Average-value equivalent models from MATLAB [37] are used to model the DC/DC converters (see Fig. 2c). Despite their simplicity, they represent quite well the dynamic behavior of the converters, and they have been used in several applications for long time simulations [42, 43]. In these models, the converters are composed of controllable voltage and current sources, whose input/output voltages and currents are related thought the duty cycle.

Furthermore, the connection with the grid is made up a voltage source inverter (VSI) and a delta-wye transformer to adapt the output voltage of the VSI to the grid voltage (see Fig. 2d). The VSI is based on the model described in [44], in which only the snubber resistance is taken into account.

IV. Decentralized Control Method (DCM) based on Fuzzy Logic Controllers

As the name of the control method suggests, in the proposed DCM, each component of the CS works independently from the rest of them. Thus, independent controllers based on fuzzy logic systems are developed for the power converters of the BESS and the grid. In the case of the PV system, it is assumed to work in the maximum power point tracking (MPPT) so that no fuzzy logic control is necessary.

The immediate purpose of this decentralized control is the control of the MVDC bus voltage and BESS SOC, keeping the power balance in the CS. Moreover, it allows an easy integration of new elements to the CS controlled by similar fuzzy systems.

Fig. 5 shows the fuzzy logic systems proposed for the BESS

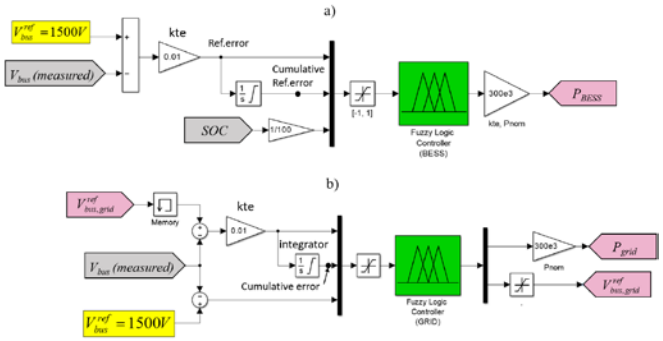

Fig. 5. Fuzzy logic systems based controllers. a) BESS power controller. b) Grid power controller.

and for the grid connection system. In both cases, the controls are based on fuzzy controllers whose outputs are the reference powers for the BESS and grid power converters.

A. Fuzzy Logic System for Controlling the BESS Power Converter

As previously mentioned, the control developed for the BESS has two objectives: to keep the MVDC bus voltage and control the BESS SOC.

The fuzzy logic system used in this converter has three inputs and one output. The inputs are the BESS SOC, the reference bus voltage error *Ref.error* (calculated as the difference between the rated value of the MVDC voltage, 1500V, and the current MVDC bus voltage) and its integral (named cumulative error). As a previous step, the error and cumulative error are normalized between -1 and 1, that correspond to values of -100V and +100V, respectively. Note that this involves that the operation limits for the MVDC bus voltage are set to 1400V and 1600V, respectively. Similarly, the BESS SOC is normalized between 0 and 1. Figs. 6a and 6b show the membership functions (MF) of the inputs. Five MFs are selected for the *Ref.error* and *cumulative Ref.error*: Negative Big (NB), Negative (N), Zero (Z), Positive (P), and Positive Big (PB). Three MFs are used in the case of the BESS SOC, which correspond to Low (L), Medium (M) or High (H).

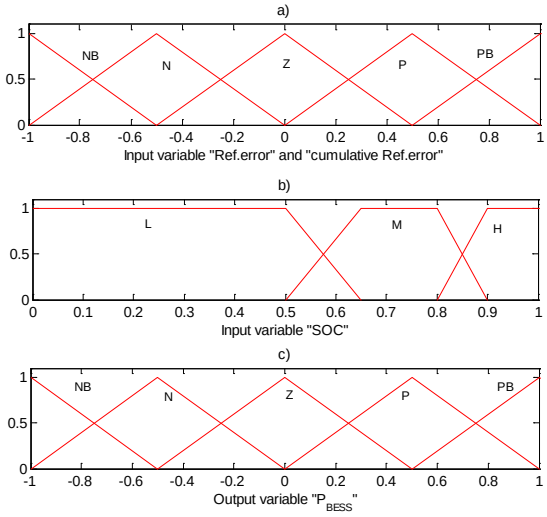

Fig. 6. Membership functions. a) Ref. error and cumulative error. b) SOC. c) BESS power (P_{BESS}).

This article has been accepted for publication in a future issue of this journal, but has not been fully edited. Content may change prior to final publication. Citation information: DOI 10.1109/JESTPE.2018.2796029, IEEE Journal of Emerging and Selected Topics in Power Electronics

On the other hand, the output of the fuzzy controller is the BESS power (P_{BESS}). The BESS power is the power that the ESS has to absorb or generate. As in the case of the inputs, this power is normalized between -1 and +1. Five MFs are considered (see Fig. 6c): Negative Big (NB), Negative (N), Zero (Z), Positive (P), and Positive Big (PB).

Table II shows the rule base of the fuzzy logic controller for the BESS power. This control modifies the BESS power when its SOC is close to a low (L) or high (H) level. The premise followed is based on the fact that when the SOC is high (H), the battery must be mainly discharged and the BESS power can only be positive, and when the SOC is low (L), following the same logic, negative. These limitations in the BESS power prioritize the control of the SOC to the MVDC bus control. It

TABLE II. RULE BASE FOR THE ESS CONTROL. OUTPUT: P_{BESS}

	Medium SOC	Cumulative Ref.error				
		NB	N	Z	P	PB
Ref. error	NB	NB	NB	NB	N	Z
	N	NB	N	N	Z	P
	Z	NB	N	Z	P	PB
	P	NB	Z	P	PB	PB
	PB	Z	P	PB	PB	PB
	High SOC	Cumulative Ref.error				
		NB	N	Z	P	PB
Ref. error	NB	Z	Z	Z	Z	Z
	N	Z	Z	Z	Z	P
	Z	Z	Z	Z	P	PB
	P	Z	Z	P	PB	PB
	PB	Z	P	PB	PB	PB
	Low SOC	Cumulative Ref.error				
		NB	N	Z	P	PB
Ref. error	NB	NB	NB	NB	N	Z
	N	NB	N	N	Z	Z
	Z	NB	N	Z	Z	Z
	P	N	Z	Z	Z	Z
	PB	Z	Z	Z	Z	Z

leads to a MVDC bus voltage fluctuation that must be managed by the grid, whose controller rules are designed under this premise.

B. *Fuzzy Logic System for Controlling the Grid Connection*

As commented at the end of the previous section, in the event that the MVDC bus voltage cannot be kept by the BESS, the grid connection system must control it. The grid fuzzy logic system generates the power that it has to absorb or generate (P_{grid}) and the reference MVDC bus voltage for the grid connection ($V^{ref}_{bus,grid}$). This controller allows keeping the power balance in the MVDC bus. It works as follows, when the reference error (*Ref.error*) is positive, it means that there is an excess of power that the grid must absorb. On the contrary, if the *Ref.error* is negative it means that there is a lack of power in the MVDC bus so the grid must inject power.

The fuzzy controller for the grid connection has three inputs and two outputs. The inputs are the error (difference between $V^{ref}_{bus,grid}$ and the current value of the MVDC bus voltage), its integral (cumulative error) and *Ref.error*. The outputs, described previously, are P_{grid} and $V^{ref}_{bus,grid}$. The MFs for the

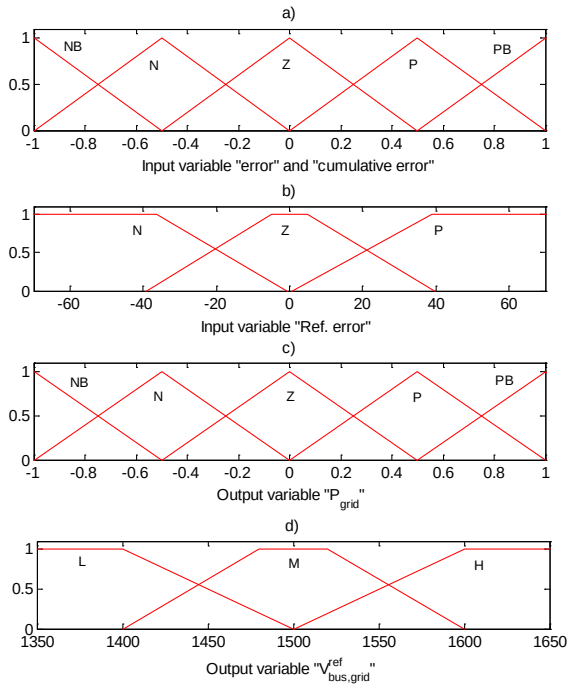

Fig. 7. Membership functions. a) Error and cumulative error (error= $V^{ref}_{bus,grid}$ -V_{bus}). b) Difference between the rated value of the MVDC voltage and its current value (*Ref. error*=1500-V_{bus}). c) Grid power (P_{grid}). d) Reference DC bus voltage for the grid connection system ($V^{ref}_{bus,grid}$ = V^{ref}_{bus}).

TABLE III. RULE BASE FOR THE GRID CONNECTION CONTROL. OUTPUTS P_{GRID} / $V^{REF}_{BUS,GRID}$

	Ref. error = Z	Cumulative Error				
		NB	N	Z	P	PB
Error	NB	Z / M	Z / M	Z / M	Z / M	Z / M
	N	Z / M	Z / M	Z / M	Z / M	Z / M
	Z	Z / M	Z / M	Z / M	Z / M	Z / M
	P	Z / M	Z / M	Z / M	Z / M	Z / M
	PB	Z / M	Z / M	Z / M	Z / M	Z / M
	Ref. error = P	Cumulative Error				
		NB	N	Z	P	PB
Error	NB	Z / L	Z / L	Z / L	Z / L	Z / L
	N	Z / L	Z / L	Z / L	Z / L	P / L
	Z	Z / L	Z / L	Z / L	P / L	PB / L
	P	Z / L	Z / L	P / L	PB / L	PB / L
	PB	Z / L	P / L	PB / L	PB / L	PB / L
	Ref. error = N	Cumulative Error				
		NB	N	Z	P	PB
Error	NB	NB / H	NB / H	NB / H	N / H	Z / H
	N	NB / H	N / H	N / H	Z / H	Z / H
	Z	NB / H	N / H	Z / H	Z / H	Z / H
	P	N / H	Z / H	Z / H	Z / H	Z / H
	PB	Z / H	Z / H	Z / H	Z / H	Z / H

error, the cumulative error and the grid power are the same as for the case of the BESS. Three MFs are used for the *Ref.error*: Negative (N), Zero (Z) and Positive (P). Finally, the MFs for the $V^{ref}_{bus,grid}$ are: Low (L), Medium (M) or High (H).

Fig. 7 shows all the MFs of this controller and Table III its rule base. Note that when *Ref.error* is Z, P_{grid} is Z and $V^{ref}_{bus,grid}$ is M. In this case, the BESS controls the MVDC bus voltage, so the grid is disconnected. On the contrary, if *Ref.error* takes a value of N or P, this means that the BESS cannot control the MVDC voltage, so the grid must be connected to the CS to control the MVDC bus voltage. Thus, if *Ref.error* is P and $V^{ref}_{bus,grid}$ is L, the grid injects to the CS

This article has been accepted for publication in a future issue of this journal, but has not been fully edited. Content may change prior to final publication. Citation information: DOI 10.1109/JESTPE.2018.2796029, IEEE Journal of Emerging and Selected Topics in Power Electronics

the lack of power needed to control the MVDC voltage. Similarly, if *Ref.error* is N and $V^{ref}_{bus,grid}$ is H, the grid absorbs the surplus power of the MVDC bus.

V. Simulation Results

This section shows the scenario considered under study, the performance of the proposed fuzzy logic based DCM, denoted as F-DCM, and a comparison with a control based on traditional controllers already presented in [45], denoted as reference-DCM (R-DCM), and a sensitive and stability analysis of the results obtained by the fuzzy logic based DCM. The considered scenario study for the comparison is carried out under MATLAB-Simulink environment and lasts more than 20 minutes.

A. Scenario Study

The scenario considered under study, sun irradiance and power demanded by the EVs, is depicted by Fig. 8a and 8b.

Fig. 8a shows the sun irradiance profile and Fig. 8b the power demanded by the EVs to the CS. It can be observed that for the first 450 seconds the irradiance is quite low (no more than 0.2 kW/m2) except between the seconds 100 and 200 (around 0.4 – 0.6 kW/m2). This fact represents cloud shading. After the second 450, the cloud vanishes and the sun irradiance noticeable increases. From this second until the second 1280 approximately, the average sun irradiance is 0.9 kW/m2. Finally, the simulation ends with a sun irradiance around 0.3 kW/m2. Regarding the power demanded, it can be noticed that the three EVs are connected at different instants to the CS. The first EV is connected at the beginning of the study, the second vehicle at the second 250 and the third one at the second 880. The maximum demanded power happens after the connection of the second EV with a value of 90 kW and when the sun irradiance is quite low. The minimum demanded load occurs in the period of time in which the sun irradiance is high. These extreme conditions have been selected to check the right performance of the fuzzy logic DCM: it will have to control the MVDC voltage keeping the power balance between the components of the CS and the EVs.

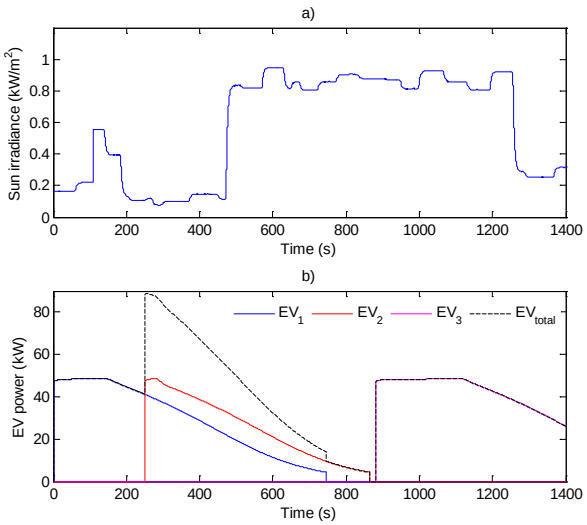

Fig. 8. a) Irradiance profile. b) Power demanded by the EV.

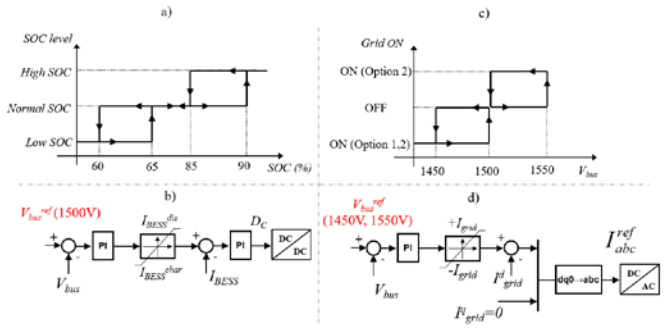

Fig. 9. R-DCM. a) Hysteresis cycles for the BESS control. b) Control scheme of the BESS converter. c) Hysteresis cycles for the reference voltage of the grid inverter. d) Control scheme of the grid inverter.

As noted above, a simpler DCM already developed in [45] is used in this paper as a reference in order to validate the fuzzy logic DCM presented in section III. Specifically, the option 2 of that control is used as the reference DCM for the comparison. Basically, the R-DCM works similarly to the fuzzy logic DCM, but in this case, PI controllers, hysteresis cycles and heuristic rules replace the proposed fuzzy controllers. As will be shown in section V, the fuzzy logic DCM will achieve better effectiveness in the control of the MVDC voltage and BESS SOC, and in the transition between the use of BESS and the grid connection.

Fig. 9a and 9b show the control schemes used in R-DCM. The values for I_{BESS}^{dis} and I_{BESS}^{char} depend on the BESS SOC. With a normal SOC (Fig. 8a), the BESS controls the DC bus voltage at 1500V (Fig. 9b) and the grid converter is disconnected. When the BESS achieves a high SOC (Fig. 9a), the BESS charging current (I_{BESS}^{char}) is limited to zero, the BESS is not able to keep the DC bus voltage at 1500 V, and then the DC bus voltage increases. When the DC bus voltage achieves 1600V, the grid converter is connected (Fig. 9c), the reference voltage of this converter changes to 1600V (V_{bus}^{ref} =1600V), and the grid is responsible for controlling the DC bus voltage at this value (Fig. 9d). When the SOC is low, the BESS discharging current (I_{BESS}^{dis}) is limited to zero. Then the DC bus voltage decreases and the grid converter is connected to keep the MVDC voltage at 1400V (V_{bus}^{ref} =1400V). Note that similarly to the BESS, the values of + I_{grid} and – I_{grid} are limited. When the V_{bus}^{ref} is 1600V, + I_{grid} takes a value of zero and when V_{bus}^{ref} is 1400V, –I_{grid} is limited to zero. In any other case, this limitation only depends on the rated power of the grid converter.

B. Performance of the EVCS and Comparative Study

This section shows the performance of the proposed fuzzy logic based DCM, denoted as F-DCM, compared with the R-DCM.

Fig. 10 represents the SOC, the input current and the voltage of the EV batteries. As observed, the three EVs are connected to the CS with different initial SOC. Depending on this SOC at the time of connection, the EV will be charged in the CCM for longer. After this period, in the three cases, the EVs are charged in the CVM. For the batteries used in this work, the charging current (I_{char}) is 120A and the charging voltage (V_{char}) 402V. Once the batteries reach this voltage, the EVs are considered fully charged if the present charge current is lower than 5% of I_{char} for 2 minutes. It can be seen the fully charging

This article has been accepted for publication in a future issue of this journal, but has not been fully edited. Content may change prior to final publication. Citation information: DOI 10.1109/JESTPE.2018.2796029, IEEE Journal of Emerging and Selected Topics in Power Electronics

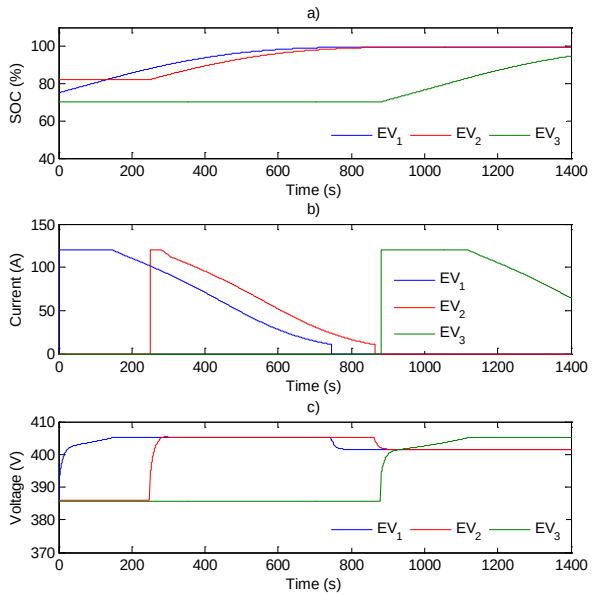

Fig. 10. EV batteries. a) SOC. b) Current. c) Voltage.

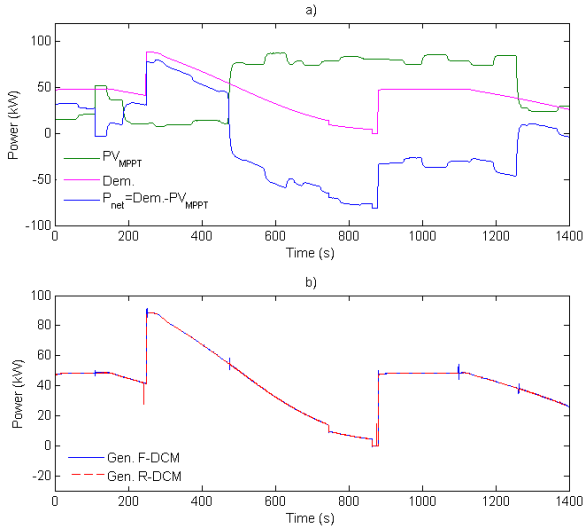

Fig. 11. a) Power generated by the PV system, total power demanded by the CS and net power. b) Total power generated by both DCMs.

process of the EV1 and the EV2 (lines blue and red) while the EV3 is not completely charged at the end of this study.

The results shown in Fig. 10 fit quite well with the ideal charging cycle presented in Fig. 4. But there are some differences that result from the performance of the presented controller. Focusing on the EV1, the CCM starts at the beginning of the simulation with a constant current of 120 A. During this stage, the voltage increases from 385 V to 405 V but, unlike the ideal charging, it varies from a high rate at the beginning of the CCM (until second 35) and then it attenuates until the end of the CCM (unlike the ideal charge in which the voltage increases at a constant rate). When the voltage reaches the requested value (405 V), the charging changes to CVM. In this mode, both ideal and the results present a similar behavior: the voltage is kept constant and the current diminishes at a decreasing rate.

The power generated by the PV system and the total power demanded by the CS (the three EVs) are shown in Fig. 11a. As commented previously, the PV system works in the MPPT in both DCM. The difference between the power demanded by the EVs and the power generated by PV (pink line minus green line) is the power to be delivered or absorbed by the BESS/grid (blue line), which is denoted as P_{net} (net power). Positive values of P_{net} mean power to be delivered and negative values to be absorbed by the BESS or the grid. Moreover, the total power generated by the CS with both controls is shown in Fig. 11b. This power corresponds to the total power demanded by the CS in Fig. 11a (pink line). The results show that both DCMs are able to supply this demanded power.

Fig. 12 represents the BESS power and the grid power during the considered scenario. These parameters are the outputs of the DCM. Fig. 12a depicts the BESS and the grid power for the F-DCM and Fig.12b for the R-DCM. Besides, Fig. 12c shows the sum between the BESS and grid power for both DCMs. It is observed that for both DCMs this power is practically the same and, at the same time, similar to the net power (blue line in Fig. 11a; subtraction between the demanded power and the PV system power), which supports the right performance of the DCM. These figures are closely related with Fig. 13, which shows the reference and the real voltage in the MVDC (Fig. 13a and Fig. 13b) and the BESS SOC for both DCMs (Fig. 13c).

The results show that when the BESS is at medium level (M in Fig. 6b) the F-DCM and the R-DCM work similarly. Under this circumstance, the main objective of both DCMs is to control the MVDC voltage keeping the power balance among the BESS, the grid (Fig. 12c), the EV chargers and the PV system (blue line in Fig. 11a). Figs. 12a and 12b show that the BESS power is the same for both DCMs in the interval between the beginning of the simulation and approximately the second 250 (it is not exactly the same time for both DCM), and then, from the second 480 to the second 850. In this period, the reference MVDC voltage is set to 1500V.

The main difference between both DCMs appears when the

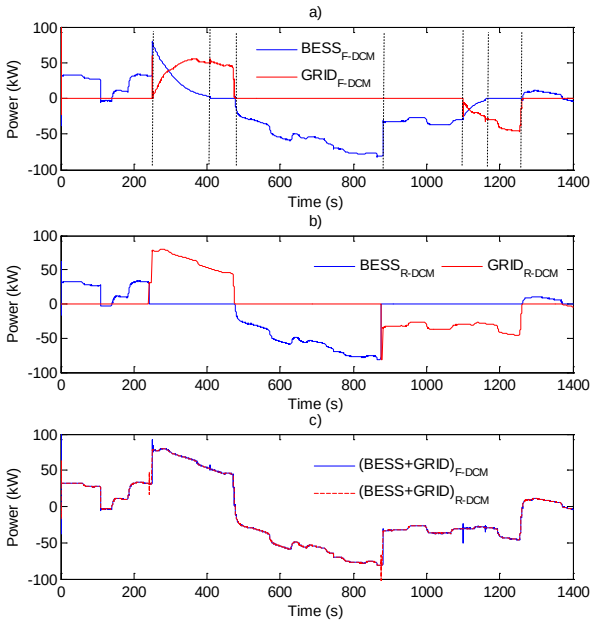

Fig. 12. a) BESS and grid powers for the F-DCM. b) BESS and grid powers for the R-DCM. c) Sum of BESS and grid power for both DCMs.

BESS SOC is close to high or low values. For example, around the second 250, the R-DCM detects that the BESS has a low SOC, the reference MVDC voltage changes to 1400V and the grid has to control this voltage, since the BESS is disconnected. In the case of the F-DCM, the fuzzy logic makes possible a smoother transition because it starts to limit the output power of the BESS due to its low SOC. Thus, because of this power limitation, the MVDC bus voltage tends to decrease. Once the MVDC voltage reaches 1400V, the fuzzy controller of the grid detects this value and sets the reference MVDC bus voltage for the grid converter ($V^{ref}_{bus,grid}$) to 1400V. Then, for an interval, although the reference voltage has changed to a value of 1400V (Fig. 13a), both the BESS and grid are controlling the MVDC bus voltage (see Fig. 12a between the second 250 and 410 approximately). After this period and up to the second 480, the BESS is disconnected and only the grid controls the MVDC voltage. From the second 480 there is an excess of power in the MVDC bus and, because of the BESS SOC is low, it can absorb it and therefore, control the bus voltage. Then, the reference voltage changes to 1500V. At the second 880, the R-DCM detects that the BESS SOC is high (red line in Fig. 13c), so that the BESS is disconnected and the excess of power is injected into the grid. Then, the reference voltage is 1600V. Regarding the F-DCM, this change is less abrupt again. For the F-DCM, the BESS SOC starts to be high around the second 1100 (blue line in Fig. 13c), and therefore, its fuzzy controller limits the input power in the BESS. This fact involves an increase in the MVDC bus voltage and when the MVDC bus voltage takes a value of 1600V, the grid fuzzy controller detects it and changes the reference voltage for the grid converter ($V^{ref}_{bus,grid}$) to 1600V. Then, again, for a brief interval of time (1100 – 1180) both, the BESS and grid, are keeping the power balance and controlling the MVDC voltage at 1600V (see Fig. 13a). After this, and up the second 1340, all the excess of power is injected into the grid.

Table IV summaries the most representative parameters obtained from the simulation. Moreover, a comparison of the MVDC voltage control using different performance indices is shown in this table. Other parameters included in this table are: *Energy demanded by the CS (kWh)*; *energy generated by the PV system (kWh)*; *energy absorbed by the FCS from the grid (kWh)*; *energy injected by the FCS (PV system) to the grid (kWh)*; *percentage of energy generated by the BESS*; *percentage of energy generated by the grid*; *percentage of energy generated by the PV system*; *percentage of time that the grid must be connected to the CS.* With respect to the performance comparison, the indices considered for the MVDC bus voltage are the following ones: *ITAE*, integral time absolute error; *ITSE*, integral time square error; *MRE*, mean relative error; and *MSE*, mean squared error.

From these results it can be drawn that, in general, the F-DCM optimizes the use of the BESS so that the CS is able to work longer off grid. This fact is supported by the time that the grid must be connected to the CS. For the F-DCM, the grid is connected during the 27.5% of the simulation and for the R-DCM, the 46.1%. Furthermore, if the CS works longer as a stand-alone system, this involves a decrease of problems related to the CS connection to the grid, such as wave quality

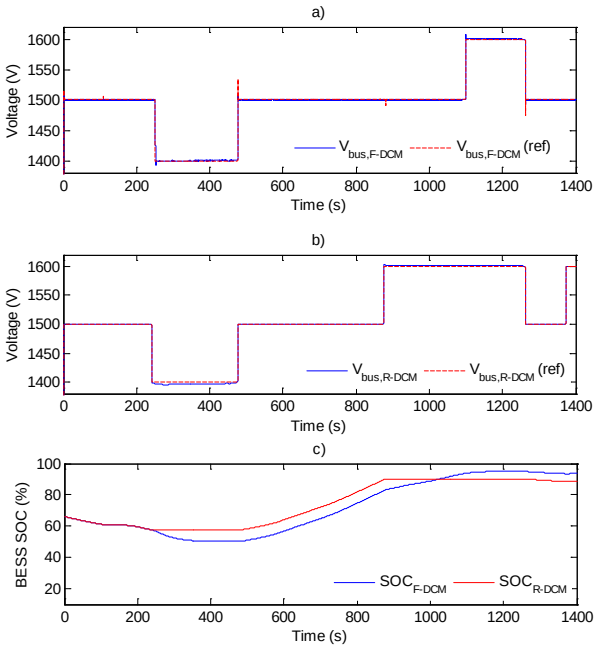

Fig. 13. a) DC bus voltage and reference voltage for the F-DCM. b) DC bus voltage and reference voltage for the R-DCM. c) BESS SOC for both DCMs.

TABLE IV.
RESULTS OF THE COMPARISON PARAMETERS OBTAINED BY EACH DCM

Parameter	***F-DCM***	***R-DCM***
Energy demanded by CS (kWh)	16,62	16,62
Energy generated by the PV system (kWh)	20,75	20,75
Energy absorbed by the fast CS from the grid (kWh)	2,71	3,95
Energy injected by the fast CS (PV system) to the grid (kWh)	1,35	3,6
% of energy generated by the ESS (%)	18,16	10,63
% of energy generated by the grid (%)	16,28	23,81
% of energy generated by the PV system (%)	65,56	65,56
$ITAE = \sum_{i=1}^{N} i \cdot \Delta t \cdot \left\lvert \left(V^{ref}_{bus}(i) - V_{bus}(i)\right)\right\rvert$	0.68x10^6	1.12x10^6
$ITSE = \sum_{i=1}^{N} i \cdot \Delta t \cdot \left(V^{ref}_{bus}(i) - V_{bus}(i)\right)^2$	3.10x10^6	5.63x10^6
$MRE = \frac{1}{N}\sum_{i=1}^{N} \frac{\left(V^{ref}_{bus}(i) - V_{bus}(i)\right)}{V_{bus}(i)}$	0.3959	0.4297
$MSE = \frac{1}{N}\sum_{i=1}^{N} \left(V^{ref}_{bus}(i) - V_{bus}(i)\right)^2$	3.44x10^3	5.01x10^3

(harmonics), fluctuations in the voltage, system stability and power outages.

It can be observed from the performance comparison of the MVDC voltage control that better results are obtained for the F-DCM. Only for the *MRE* the final result is quite similar.

C. Sensitivity and Stability Analysis

Finally, with the aim of completing the study of the proposed fuzzy logic DCM, performing a sensitivity and stability analysis and showing how the components of the system interact, other two types of simulations are carried out. The first of them consists of a set of Monte Carlo simulations (two hundred simulations of ten second each), in which the input parameters of the proposed control (initial BESS SOC, PV system power, and numbers of EVs connected to the CS)

This article has been accepted for publication in a future issue of this journal, but has not been fully edited. Content may change prior to final publication. Citation information: DOI 10.1109/JESTPE.2018.2796029, IEEE Journal of Emerging and Selected Topics in Power Electronics

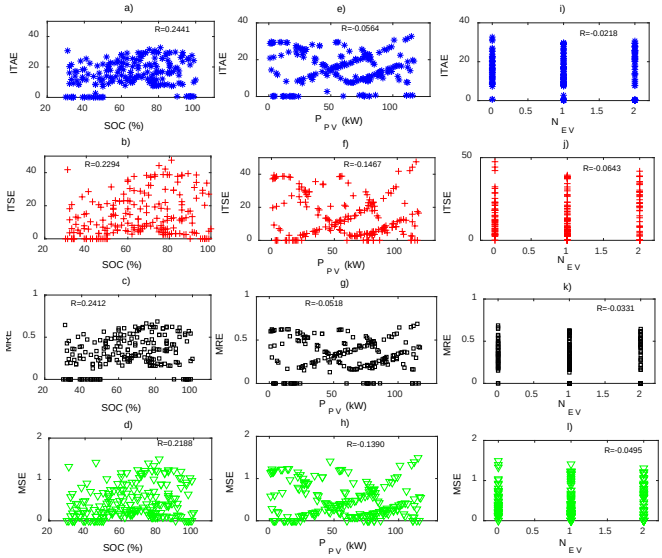

Fig. 14. Results of the Monte Carlo simulations. a) ITAE vs SOC. b) ITSE vs SOC. c) MRE vs SOC. d) MSE vs SOC. e) ITAE vs P_{pv}. f) ITSE vs P_{pv}. g) MRE vs P_{pv}. h) MSE vs P_{pv}. i) ITAE vs NEV. j) ITSE vs NEV. k) MRE vs NEV. l) MSE vs NEV.

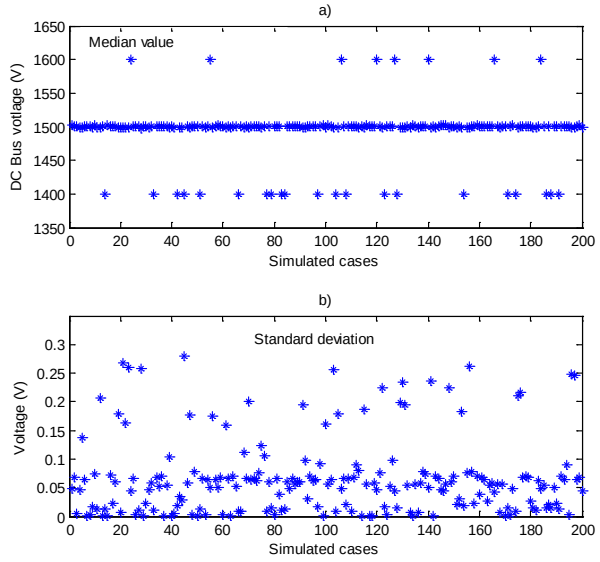

Fig. 15. Results of the Monte Carlo simulations for the MVDC bus voltage. a) Median value. b) Standard deviation.

are modified randomly in order to know the control results and the response of the whole system under study. The value of the performance indices (ITAE, ITSE, MRE and MSE), the median value and the standard deviation of the DC bus voltage are calculated and analyzed in order to evaluate the control system. The other simulation consists of three simulations of 120 seconds each with a specific level of SOC (low, high and normal). For each level of SOC, the cases with maximum and minimum power of the PV system (120 and 0 kW), and without EVs and with two EVs connected to the CS are studied. Results obtained from the Monte Carlo simulation are shown in Fig. 14 and 15, whereas the results from the second simulation are depicted in Fig. 16.

Note in Fig. 14 that all the performance indices are kept around the same values. In all the considered scenarios, the DC bus voltage is maintained stable around the desired value.

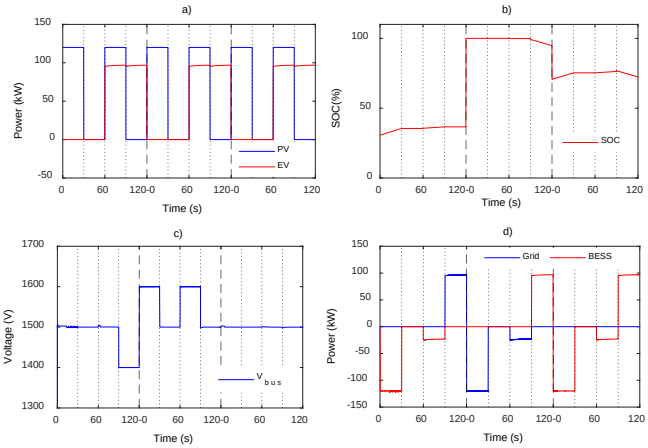

Fig. 16. Results of specific cases of the Monte Carlo simulations. a) PV power and EVs power. b) BESS SOC. c) MVDC bus voltage. d) Grid and BESS powers.

These output values correspond to the system response under randomly generated inputs. The SOC is randomly generated between 30% and 100% (Fig. 14a-14d), the PV system between the 0 and 120kW (Fig. 14e-14h), and the number of EVs connected only can take three values, 0, 1 or 2 (Fig. 14i-14l). The results show a very slight linear correlation between the BESS SOC and the performance indices. Regarding the PV system power and number of EVs connected to the CS this correlation is even smaller. The stability of the MVDC bus voltage can be also verified in Fig. 15. The median value and the standard deviation of the MVDC bus voltage are shown in Fig 15a and 15b. Again, this voltage is kept controlled around the desired value in all the simulated cases (1500V for normal SOC, 1400V for a low SOC and 1600V for a high SOC) and with a very low a standard deviation.

Fig. 16 shows the results obtained for the PV and EVs powers, BESS SOC, MVDC bus voltage, and grid and BESS powers in some specific cases of the Monte Carlo simulations performed. The inputs are: the PV system power (0 or 120kW), the power demanded by the EVs (0 or 2 EVs) and the BESS SOC (30%, 100% and 70%). This figure shows how the converters interact knowing only the voltage level of the DC bus. Thus, when the battery SOC is low, there is no power supply from the PV system and there are two EVs connected, the DC bus voltage has a value of 1400V and all the power demanded by the EVs must be provided by the grid. On the contrary, if the battery SOC is high and there is an excess of power generated by the PV system, the DC bus voltage is kept at 1600V and this excess of power is injected into the grid. In any case, the battery is able to control the DC bus voltage at 1500V. As can be observed, the proposal control methodology is decentralized, so there is not any information exchange between the DC/DC converters, and the working point of the CS is given by the voltage level of the MVDC bus.

VI. Conclusion

Generally, in the field of the renewable hybrid systems, fuzzy logic has been used for the management of the energy among their components or as controller in the power electronic converters. This paper has presented, as main contribution, a novel decentralized control combining both

uses of the fuzzy logic for a CS with renewable energy and energy storage, in which fuzzy logic controllers were used as a decentralized EMS to control the converters of two components of the system separately and achieve a coordinated performance operation of the following system parameters: power flow, MVDC voltage and BESS SOC. Another novelty was to include the SOC of the BESS as a control variable for a decentralized EMS (that is very common for centralized approaches but, as the literature review showed, not for decentralized ones). Moreover, the different power converters were modelled as average models that result in simulations that represent more reliably the CS dynamics improving the approaches followed before in this area (based on quasi dynamic simulations and neglecting power converters). Finally, the novel decentralized control was evaluated and analyzed in a considerable number of operating situations by Monte Carlo simulations, in contrast to the previous works published on this topic, in order to perform a sensitivity and stability analysis of the proposed control technique and show how the elements of the system interact.

The considered CS was composed of a PV system, a battery as ESS, a connection with the local grid and two units of fast charging for EVs. Two fuzzy logic systems (one for the BESS and other for the grid connection) were implemented as controllers for the control of MVDC voltage and the BESS SOC and for the management of the input and output powers among all the components, meanwhile the PV system was working in the MPPT.

The fuzzy logic systems implemented in this work (F-DCM) were able to control the MVDC and the power flow among the components of the fast CS without the need of communication. The fuzzy logic systems worked independently of each other and they adjusted the MVDC bus voltage depending on the BESS SOC.

The proposed fuzzy logic DCM was compared to a reference DCM (R-DCM) also based on a decentralized typology but with the need of using PI controllers, hysteresis cycles and heuristic rules. In addition to the advantages of a decentralized control, such as, the facility to integrate (BESS, EV charges…) without communication system among them, the fuzzy logic DCM presented several advantages respect to the reference DCM, some of them due to the combination of uses of the fuzzy logic. With the new DCM, the fast CS was able to work in a stand-alone mode longer, so problems related with the grid connection can be reduced and the use of the BESS was improved.

The Monte Carlo simulations, in which the input parameters of the control system were modified randomly, showed that, in all the considered scenarios (two hundred cases studied), the system was kept stable, the DC bus voltage was controlled at the desired value according to the BESS SOC (1500V with normal SOC, 1400V with a low SOC and 1600V with a high SOC), and the components of the CS interact successfully knowing only the voltage level of the MVDC bus.

The results demonstrated that the fuzzy logic DCM achieved better results in the controlled variables and in the response of the whole system under study, while smoothing the operation transition of the CS components (the connection and disconnection of the components to the MVDC bus) with regard to classical controllers.

REFERENCES

[1] "Key World Energy Statistics 2014," International Energy Agency (IEA), 2014. [Online]. Available: http://www.iea.org/publications/freepublications/publication/keyworld2014.pdf.

[2] "Reduction of pollutant emissions from light vehicles," EUR-lex, 2014. [Online]. Available: http://eur-lex.europa.eu/legal-content/EN/TXT/HTML/?uri=URISERV:l28186&from=EN.

[3] P. Goli and W. Shireen, "PV powered smart charging station for PHEVs," *Renew Energy*, vol. 66, pp. 280–287, Jun. 2014.

[4] L. Kütt, E. Saarijärvi, and M. Lehtonen, "A Review of the harmonic and unbalance effects in electrical distribution networks due to EV charging," in *Proc. EEEIC*, Wroclaw, Poland, May 2013. pp. 556 – 561.

[5] K. Clement-Nyns, E. Haesen, and J. Driesen, "The impact of charging plug-in hybrid electric vehicles on a residential distribution grid," *IEEE Trans. Power Syst.*, vol. 25, no. 1, pp. 371–380, Feb. 2010.

[6] L. P. Fernandez, T. G. S. Román, R. Cossent, C. M. Domingo, and P. Frias, "Assessment of the impact of plug-in electric vehicles on distribution networks," *IEEE Trans Power Syst*, vol. 26, no. 1, pp. 206–213, Feb. 2011.

[7] D. Sbordone, I. Bertini, B. Di Pietra, M. C. Falvo, A. Genovese, and L. Martirano, "EV fast charging stations and energy storage technologies: A real implementation in the smart micro grid paradigm," *Electr Pow Syst Res*, vol. 120, pp. 96–108, March 2015.

[8] J. De Santiago, H. Bernhoff, B. Ekergård, S. Eriksson, S. Ferhatovic, R. Waters, S. Member, and M. Leijon, "Electrical motor drivelines in commercial all-electric vehicles: A review," *IEEE Trans. Veh. Technol.*, vol. 61, no. 2, pp. 475–484, Feb. 2012.

[9] International Electrotechnical Commission. IEC 61851-1:2010 Electric vehicle conductive charging system - Part 1: General requirements. 2016.

[10] P. You, Z. Yang, M. Y. Chow, and Y. Sun, "Optimal cooperative charging strategy for a smart charging station of electric vehicles," *IEEE Trans. Power Syst.*, vol. 31, no. 4, pp. 2946–2956, Jul. 2016.

[11] Q. Wang, I. Safak Bayram, F. Granelli, and M. Devetsikiotis, "Fast power charging strategy for EV/PHEV in parking campus with deployment of renewable energy," *Proc. IEEE-CAMAD*, Athens, Greece. Dec. 2014, pp. 370–374.

[12] A. Y. S. Lam, K. C. Leung, and V. O. K. Li, "Capacity estimation for vehicle-to-grid frequency regulation services with smart charging mechanism," *IEEE Trans. Smart Grid*, vol. 7, no. 1, pp. 156–166, Jan. 2016.

[13] C. Sabillon Antunez, J. F. Franco, M. J. Rider, and R. Romero, "A new methodology for the optimal charging coordination of electric vehicles considering vehicle-to-grid technology," *IEEE Trans. Sustain. Energy*, vol. 7, no. 2, pp. 596–607, April 2016.

[14] A. Mohamed, V. Salehi, T. Ma, and O. Mohammed, "Real-Time Energy Management Algorithm for Plug-In Hybrid Electric Vehicle Charging Parks Involving Sustainable Energy," *IEEE Trans. Sustain. Energy*, vol. 5, no. 2, pp. 577-586, April 2014.

[15] E. H. El-Zohri and K. Sayed, "Control of EV charging station based on three-phase three-level AC/DC rectifier," *in Proc. IEEE Int. Telecommun. Energy Conf.* Osaka, Japan, Oct. 2015, pp. 1–6.

[16] L. Tan, B. Wu, V. Yaramasu, S. Rivera, and X. Guo, "Effective voltage balance control for bipolar-DC-bus fed EV charging station with three-level DC-DC fast charger," *IEEE Trans. Ind. Electron.*, vol. 46, no. 7, pp. 4031–4041, Jul. 2016.

[17] L. Tan, B. Wu, S. Rivera, and V. Yaramasu, "Comprehensive DC power balance management in high-power three-level DC-DC converter for electric vehicle fast charging," *IEEE Trans. Power Electron.*, vol. 31, no. 1, pp. 89–100, Jan. 2016.

[18] G. Preetham and W. Shireen, "Photovoltaic charging station for Plug-In Hybrid Electric Vehicles in a smart grid environment," in *IEEE PES Innovative Smart Grid Technologies* (ISGT), Jan. 2012, pp. 1–8.

[19] N. Liu, Q. Chen, X. Lu, J. Liu, and J. Zhang, "A Charging Strategy for PV-Based Battery Switch Stations Considering Service Availability and Self-Consumption of PV Energy," *IEEE Trans. Ind. Electron.*, vol. 62, no. 8, pp. 4878–4889, 2015.

[20] T. Dragičević, S. Sučić, J. C. Vasquez, and J. M. Guerrero, "Flywheel-based distributed bus signalling strategy for the public fast charging station," *IEEE Trans. Smart Grid*, vol. 5, no. 6, pp. 2825–2835, Nov. 2014.

[21] Y. Liu, Y. Tang, J. Shi, X. Shi, J. Deng, and K. Gong, "Application of small-sized SMES in an EV charging station with DC bus and PV system," *IEEE Trans. Appl. Supercond.*, vol. 25, no. 3, Jun. 2015.

[22] M. O. Badawy and Y. Sozer, "Power Flow Management of a Grid Tied PV- Battery Powered Fast Electric Vehicle charging station power flow management of a grid tied PV-battery powered fast electric vehicle charging station," in *Proc. IEEE-ECCE*, Montreal, Canada, March 2015, pp. 4959–4966.

[23] Wenhao Zhou, M. Li, He Yin, and C. Ma, "An adaptive fuzzy logic based energy management strategy for electric vehicles," *in Proc. IEEE ISIE*, Istambul, Turkey, Jul. 2014. pp. 1778–1783.

[24] S. G. Li, S. M. Sharkh, F. C. Walsh, and C. N. Zhang, "Energy and battery management of a plug-in series hybrid electric vehicle using fuzzy logic," *IEEE Trans. Veh. Technol.*, vol. 60, no. 8, pp. 3571–3585, Oct. 2011.

[25] M. A. Silva, H. N. De Melo, J. P. Trovao, P. G. Pereirinha, and H. M. Jorge, "An integrated fuzzy logic energy management for a dual-source electric vehicle," in *Proc. IEEE-IECON*. Vienna, Austria, Nov. 2013. pp. 4564–4569,

[26] L. Yao, Z. Damiran, and W. H. Lim, "A fuzzy logic based charging scheme for electric vechicle parking station," in *Proc. IEEE-EEEIC*, Florence, Italy, Jun. 2016. pp. 1-6

[27] W. Chen, L. Wang, A. Ulatowski, and A. M. Bazzi, "A fuzzy logic approach for fault diagnosis and recovery in PHEV and EV chargers," in *Proc. IEEE Transp. Electrif. Conf. Expo*, Florence, Italy, Dec. 2014. pp. 1–5

[28] M. A. Hannan, Z. A. Ghani, A. Mohamed, and M. N. Uddin, "Real-time testing of a fuzzy logic controller based grid-connected photovoltaic inverter system," *IEEE Trans. Ind. Appl.*, vol. 51, no. 6, pp. 4775–4784, Nov-Dec. 2015.

[29] K. Thirugnanam, "Fuzzy based active and reactive power support to the distribution network using electric vehicles." in *Proc. IEEE-ITEC*, Chennai, India, Aug. 2015, pp. 1-6.

[30] T. P. Ezhil Reena Joy, K. Thirugnanam, and P. Kumar, "A new concept for bidirectional inductively coupled battery charging system based on AC-DC-AC converter for PHEV's and EV's using fuzzy logic approach," *in Proc. IEEE Transp. Electrif. Conf. Expo.*, Miami, USA, Jun. 2012, pp. 0–5.

[31] Suntech-Power, "265 Watt," *STP265-20/Wem(265_260_255)*, 2016. [Online]. Available: http://www.suntech-power.com/menu/suntech-products.html.

[32] Discover Energy. Corp., "48V 2.0 kWh Advanced Energy System (AES)," 2015. [Online]. Available: http://discover-energy.com/product-search/view/13-48-2000.

[33] Xalt Energy, "XALT® 31 Ah High Energy (HE) Superior Lithium Ion Cell," 2015. [Online]. Available: http://www.xaltenergy.com/images/pdfs/datasheets/XALT_SpecSheet_R_31Ah_HE.pdf.

[34] T. Luo, M. J. Dolan, E. M. Davidson, and G. W. Ault, "Assessment of a new constraint satisfaction-based hybrid distributed control technique for power flow management in distribution networks with generation and demand response," *IEEE Trans. Smart Grid*, vol. 6, no. 1, pp. 271–278, Jan. 2015.

[35] M. Hosseini, I. Dincer, and M. A. Rosen, "Hybrid solar–fuel cell combined heat and power systems for residential applications: Energy and exergy analyses," *J. Power Sources*, vol. 221, pp. 372–380, Jan 2013.

[36] A. M. Humada, M. Hojabri, S. Mekhilef, and H. M. Hamada, "Solar cell parameters extraction based on single and double-diode models: A review," *Renewable and Sustainable Energy Reviews*, vol. 56, pp. 494-509, 2016.

[37] *SimPowerSystems*, Reference. Hydro-Québec and the MathWorks," Inc., Natick, MA, 2015.

[38] Tremblay, O., L.-A. Dessaint, "Experimental Validation of a Battery Dynamic Model for EV Applications," *World Electric Vehicle Journal*, vol. 3, pp. 1-10, May 2009.

[39] A. Berrueta, I. S. Martín, P. Sanchis and A. Ursúa, "Comparison of State-of-Charge estimation methods for stationary Lithium-ion batteries," IECON 2016 - 42nd Annual Conference of the IEEE Industrial Electronics Society, Florence, 2016, pp. 2010-2015.

[40] J. Y. Yong, V. K. Ramachandaramurthy, K. M. Tan, and N. Mithulananthan, "Bi-directional electric vehicle fast charging station with novel reactive power compensation for voltage regulation," *Int. J. Elec. Power*, vol. 64, pp. 300–310, Jan. 2015.

[41] J. Zhong, L. He, C. Li, Y. Cao, J. Wang, B. Fang, L. Zeng, and G. Xiao, "Coordinated control for large-scale EV charging facilities and energy storage devices participating in frequency regulation," *Appl. Energy*, vol. 123, pp. 253–262, Jun. 2014.

[42] M. K. Kazimierczuk, *Pulse-width modulated DC-DC power converters*. Chichester, UK: John Wiley & Sons, 2008.

[43] A. J. Sabzali, E. H. Ismail, and H. M. Behbehani, "High voltage step-up integrated double Boost–Sepic DC–DC converter for fuel-cell and photovoltaic applications," *Renew. Energy*, vol. 82, pp. 44–53, Oct. 2015.

[44] I. Vechiu, O. Curea, and H. Camblong, "Transient Operation of a Four-Leg Inverter for Autonomous Applications With Unbalanced Load," *IEEE Transactions on Power Electronics*, vol. 25(2), pp. 399-407, Feb. 2010.

[45] P. García-Triviño, J. P. Torreglosa, L. M. Fernández-Ramírez, and F. Jurado, "Control and operation of power sources in a medium-voltage direct-current microgrid for an electric vehicle fast charging station with a photovoltaic and a battery energy storage system," *Energy*, vol. 115, pp. 38–48, Nov. 2016.

Pablo García-Triviño was born in La Linea de la Concepcion (Cádiz), Spain, in 1984. He received the MSc degree in Engineering from the University of Cadiz, Spain, in 2007, and the Ph.D. degree from the University of Cadiz, Spain, in 2010.
Since 2008, he is an Associate Professor at the Department of Electrical Engineering of the University of Cadiz, Spain. His research interest focuses on power systems and power management in hybrid systems.

Juan P. Torreglosa was born in Sevilla, Spain, in 1985. He received the M.Sc. degree in industrial engineering and Ph.D. degree from the University of Jaén, Jaén, Spain, in 2009 and 2012, respectively.
He has worked as a Researcher in different projects at the University of Jaen since 2009. From 2015, he is an Assistant Professor at the Electrical Engineering Department of the University of Huelva, Spain. His research activities are mainly focused on energy management applied to hybrid systems composed by renewable energy sources.

Luis M. Fernández-Ramírez (M'11-SM'15) was born in Los Barrios (Cadiz), Spain. He received the M.Sc. degree in electrical engineering from the University of Seville, Seville, Spain, in 1997 and the Ph.D. degree from the University of Cadiz, Cadiz, Spain, in 2004.

From 1997 to 2000, he was with the Department of Development and Research, Desarrollos Eolicos S.A. In 2000, he joined the University of Cadiz, Spain, where he is currently an Associate Professor in the Department of Electrical Engineering and Head of the Research Group in Electrical Technologies for Sustainable and Renewable Energy (PAIDI-TEP023). His current research interests include renewable energy sources and fuel cell systems.

Francisco Jurado (M'00-SM'06) was born in Linares (Jaen), Spain. He received the M.Sc. and Dr. Ing. degrees from the National University of Distance Education, Madrid, Spain, in 1995 and 1999, respectively.

Since 1985, he is a Professor with the Department of Electrical Engineering, University of Jaen, Linares, Spain. His research activities have been devoted to several topics, e.g., power systems, modeling, and renewable energy.